Structure and Properties of an Amorphous Metal-Organic Framework

Thomas D. Bennett,[1] Andrew L. Goodwin,[2,3] Martin T. Dove,[2] David A. Keen,[4,5] Matthew G. Tucker,[4] Emma R. Barney,[4] Alan K. Soper,[4] Erica G. Bithell,[1] Jin-Chong Tan,[1] and Anthony K. Cheetham[1,*]

[1]*Department of Materials Science, University of Cambridge, Cambridge CB2 3QZ, United Kingdom*
[2]*Department of Earth Sciences, Cambridge University, Downing Street, Cambridge CB2 3EQ, United Kingdom*
[3]*Department of Chemistry, University of Oxford, South Parks Road, Oxford OX1 3QR, United Kingdom*
[4]*ISIS Facility, Rutherford Appleton Laboratory, Harwell Science and Innovation Campus, Didcot, Oxfordshire OX11 0QX, United Kingdom*
[5]*Department of Physics, Oxford University, Clarendon Laboratory, Parks Road, Oxford OX1 3PU, United Kingdom*
(Received 8 January 2010; published 19 March 2010)

ZIF-4, a metal-organic framework (MOF) with a zeolitic structure, undergoes a crystal–amorphous transition on heating to 300 °C. The amorphous form, which we term a-ZIF, is recoverable to ambient conditions or may be converted to a dense crystalline phase of the same composition by heating to 400 °C. Neutron and x-ray total scattering data collected during the amorphization process are used as a basis for reverse Monte Carlo refinement of an atomistic model of the structure of a-ZIF. The structure is best understood in terms of a continuous random network analogous to that of a-SiO$_2$. Optical microscopy, electron diffraction and nanoindentation measurements reveal a-ZIF to be an isotropic glasslike phase capable of plastic flow on its formation. Our results suggest an avenue for designing broad new families of amorphous and glasslike materials that exploit the chemical and structural diversity of MOFs.

Amorphous materials are found extensively in the fields of intermetallic [1], inorganic [2], and organic materials [3], and have a wide range of important applications. Over the last 5–10 years, the materials science community has studied extensively a fourth class of materials, namely, metal-organic frameworks (MOFs) [4,5]. These are network structures in which metal atoms are linked via organic ligands in a crystalline array. Their structures can be dense or porous, and, by virtue of their combined structural and chemical versatility, they have a wide range of applications, including gas sorption and separation, magnetism and photoluminescence. While amorphous products have been identified in this emerging area [6–8]—including a very recent report of pressure-induced amorphization [9]—there are no well-characterized examples. The zeolitic imidazolate frameworks (ZIFs) [10–12] are interesting candidates for amorphization because their structures are closely related to zeolitic silica polymorphs by virtue of their analogous tetrahedral connectivites [Fig. 1]. We show here that ZIFs can form network glasses with silica-glasslike forms. Our results demonstrate how the chemical versatility of MOFs might be coupled with the attractive mechanical, optical, and electronic properties of the amorphous state to yield a new generation of advanced functional materials.

Inorganic zeolites can transform to amorphous structures with either pressure or temperature [13]. In the present work, we have discovered that the zinc imidazolate ZIF-4 [14] will amorphize at ambient pressure on heating. Bulk samples of ZIF-4 were prepared via solvothermal reaction of zinc(II) nitrate hexahydrate and imidazole in dimethylformamide (DMF) [14,15]. Thermogravimetric

analysis and variable-temperature x-ray and neutron diffraction data show that the as-prepared phase, which contains DMF molecules within its pore structure, loses this DMF on heating above 200 °C, giving a solvent-free nanoporous phase of composition Zn(im)$_2$ (im$^-$ = imidazolate anion) while maintaining the ZIF-4 topology. Further heating to 300 °C causes an irreversible transformation to an amorphous phase (referred to here as a-ZIF), indicated by the loss of all Bragg reflections in the diffraction pattern. This phase is recoverable to ambient temperature with no change in its diffraction pattern. On further heating to 400 °C, the densest of the known crystalline Zn(im)$_2$ phases (ZIF-zni) [10] evolves from the amorphous solid and is stable to around 500 °C, whereupon thermal decomposition takes place. The transformation of ZIF-4 to ZIF-zni is consistent with the lower energy of the latter calculated using *ab initio* methods [16]. While the existence of other amorphous transition-metal imidazolates has been documented [8,9,17,18], the special point here is that the thermal stability field of a-ZIF is bounded by crystalline phases of the same composition Zn(im)$_2$, removing
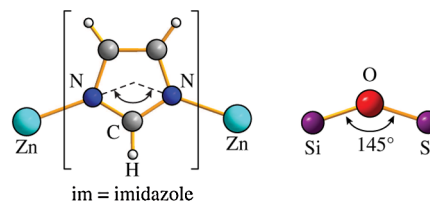

FIG. 1 (color online).   Representations of the Zn-im-Zn and Si-O-Si linkages in tetrahedral ZIF and silicate networks, respectively.

any ambiguities of composition during structure determination.

In order to probe the detailed structure of *a*-ZIF, we prepared a perdeuterated sample of ZIF-4 and collected neutron total scattering data at a number of temperatures using the GEM diffractometer at the ISIS spallation source [19]. Neutron powder diffraction patterns of the desolvated (300 °C) ZIF-4 phase, the as-prepared amorphous phase (320 °C), and the recrystallized ZIF-zni phase (400 °C) are shown in Fig. 2(a). Following appropriate normalization (see SI), the data were converted to the corresponding pair distribution functions (PDFs) [Fig. 2(b)]. Further structural data were collected for the *a*-ZIF and ZIF-zni phases using Ag Kα x-ray radiation ($\lambda = 0.561$ Å) [20]; the complete set of x-ray total scattering patterns and their corresponding Fourier transforms (i.e., effective PDFs [21]) are given as SI.

The most striking feature of the PDFs—both neutron and x-ray—is that they are virtually identical for ZIF-4, *a*-ZIF, and ZIF-zni up to approximately 6 Å [see inset to Fig. 2(b) and SI], confirming that the tetrahedral Zn coordination environment and the bridging coordination motif of the imidazolate ions [Fig. 1] are common to all three phases. We note that there is some slight broadening of the peaks in the PDFs with increasing temperature as is consistent with increased thermal motion. The PDFs begin to differ at larger distances with evidence for different medium-range order (MRO) in all three phases over distances of 10–20 Å. Peaks characteristic of crystalline order
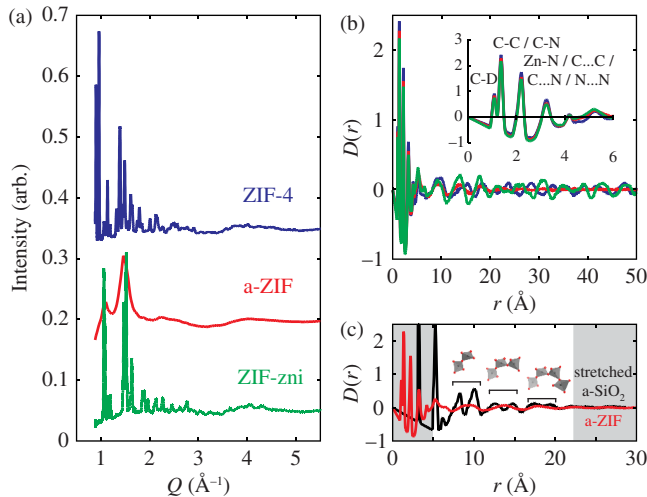
persist in the PDFs of ZIF-4 and ZIF-zni for $r > 20$ Å, whereas the PDF of *a*-ZIF is essentially featureless after $r \simeq 25$ Å. A very similar comparison can be drawn between crystalline silica polymorphs and amorphous silica (*a*-SiO$_2$) [22], where the lower critical lengthscales reflect the shorter distance between tetrahedral centers ($d_{\text{Si}...\text{Si}} \simeq$ 3.1 Å; cf. $d_{\text{Zn}...\text{Zn}} \simeq 5.9$ Å for Zn–im–Zn). Indeed, there are strong qualitative similarities in the PDFs of *a*-SiO$_2$ and *a*-ZIF at longer distances [Fig. 2(c)] that add further weight to the analogy often drawn between ZIFs and silicate analogues [14].

Detailed insight into the structure of *a*-ZIF was obtained via reverse Monte Carlo (RMC) refinement using the pro-

FIG. 2 (color online). (a) Low-*Q* ($Q < 5.5$ Å^{-1}) region of the neutron total scattering patterns of (top) the desolvated ZIF-4 framework at 300 °C, (middle) the *in situ* amorphized *a*-ZIF product at 320 °C, and (bottom) subsequently recrystallized ZIF-zni at 400 °C. (b) Neutron differential correlation functions $D(r)$ [21]; the inset illustrates the practically identical local structure in all phases. (c) $D(r)$ functions compared for *a*-ZIF and *a*-SiO$_2$ [28], where the latter data have been stretched in *r* by a factor of two to reflect approximately the difference in Zn...Zn and Si...Si distances in the two materials.
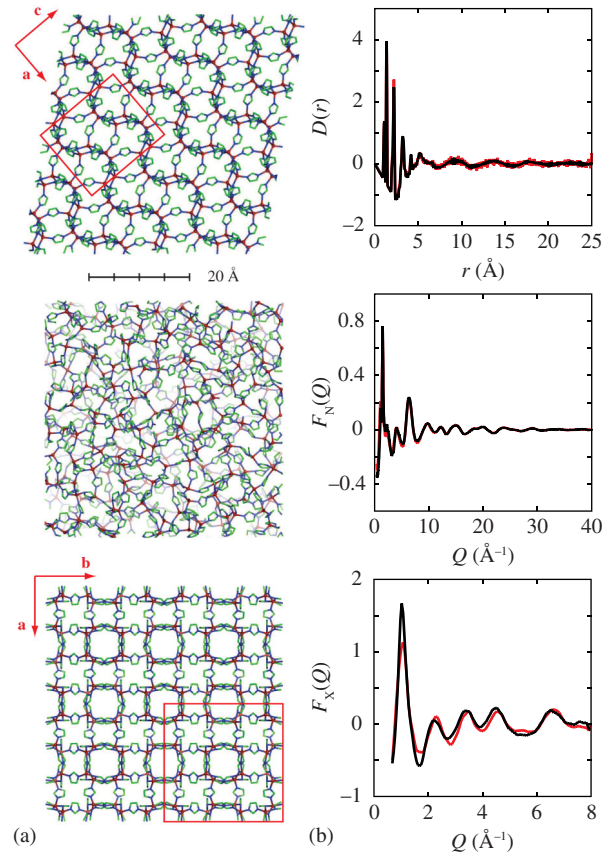

FIG. 3 (color online). (a) A region of the final RMC model of *a*-ZIF (center) shown relative to comparable regions of the ZIF-4 (top) and ZIF-zni (bottom) framework structures; the corresponding unit cells are shown in outline. Deuterium atoms have been omitted for clarity. (b) RMC fits (thin red lines) to experimental total scattering data (thicker black lines), calculated using the single atomistic configuration illustrated in the center panel of (a): (top) Neutron differential correlation function $D(r)$, (center) neutron total scattering structure factor $F_{\text{N}}(Q)$, and (bottom) x-ray total scattering structure function $F_{\text{X}}(Q)$ [21]. Although the level of agreement with the x-ray data is slightly lower than for the neutron data, we did not adjust weightings to force an improved agreement because we judge the neutron data and corresponding corrections to be of higher quality.

gram RMCPROFILE [23]. RMC modelling of crystalline-amorphous transitions in zeolites [24] and the open-framework material ZrW_2O_8 [25] has shown framework connectivity is commonly preserved during framework amorphization. Consequently, our initial starting models were based on the crystalline topologies of either ZIF-4 or ZIF-zni frameworks. We found RMC refinements that used these models were not capable of reproducing both neutron and x-ray scattering data, even after incorporation of substantial disorder of the imidazolate linkages during refinement (see SI for further details). The key implication of this result is that there must be a series of changes in connectivity within the $Zn(im)_2$ framework during both the conversion from ZIF-4 to a-ZIF and then again from a-ZIF to ZIF-zni. Indeed, this is consistent with the changes in MRO evident in the PDF data themselves [Fig. 2(b)] and also that ZIFs are known to undergo reconstructive rather than displacive transitions under application of modest pressures [26,27].

Motivated by the correspondence between features in the PDFs of a-SiO_2 and a-ZIF [Fig. 2(c)], we created a starting model for RMC by adapting a well-tested continuous random network (CRN) model of a-SiO_2 [28,29], replacing Si by Zn and oxygen by imidazolate in the appropriate orientation. This led to markedly improved fits to data, with the final RMC configuration [Fig. 3(a)] reproducing all key aspects of the experimental data [Fig. 3(b)]. The RMC procedure did not require any changes in the topology of the underlying CRN. This is strong evidence that the structure of a-ZIF is well de-scribed by a CRN of tetrahedral Zn centers connected via imidazolate linkages. While the CRN of a-SiO_2 probably has different "ring statistics" to that of a-ZIF—both ZIF-4 and ZIF-zni networks contain a relatively large number of four-membered rings, while our model of a-SiO_2 has none—so far our RMC modelling does not appear to be sufficiently sensitive to these subtleties. We can nevertheless state with confidence that the network topology in a-ZIF is disordered rather than crystal-like: the material is "truly" amorphous with a CRN topology, and not a highly disordered network solid with a crystal-like topology.

Further evidence for glasslike behavior in a-ZIF comes from optical microscopy. Crystals of ZIF-4 deform, but do not shatter, on the transition to a-ZIF [Figs. 4(a) and 4(b)]. Quite remarkably the monolithic "crystals" evolve curved internal cavities (presumably coupled with loss of included DMF) in addition to curved external morphologies across the transition [Figs. 4(b) and 4(d)], indicating that a-ZIF appears to exhibit viscous flow on its formation at 300 °C. Optical micrographs of partially transformed crystals show that the subsequent transition from a-ZIF to ZIF-zni then occurs via nucleation at surface defects [Figs. 4(d) and 4(e)]. Electron diffraction patterns collected from the amorphous phase indicate it to be isotropic [Fig. 4(f)], with no residual texture from the anisotropic ZIF-4 parent phase [Fig. 4(g)]. We also note that microcrystalline-type contrast behavior was not seen in the electron diffraction, and the amorphous diffraction pattern, which agrees very closely with the neutron and
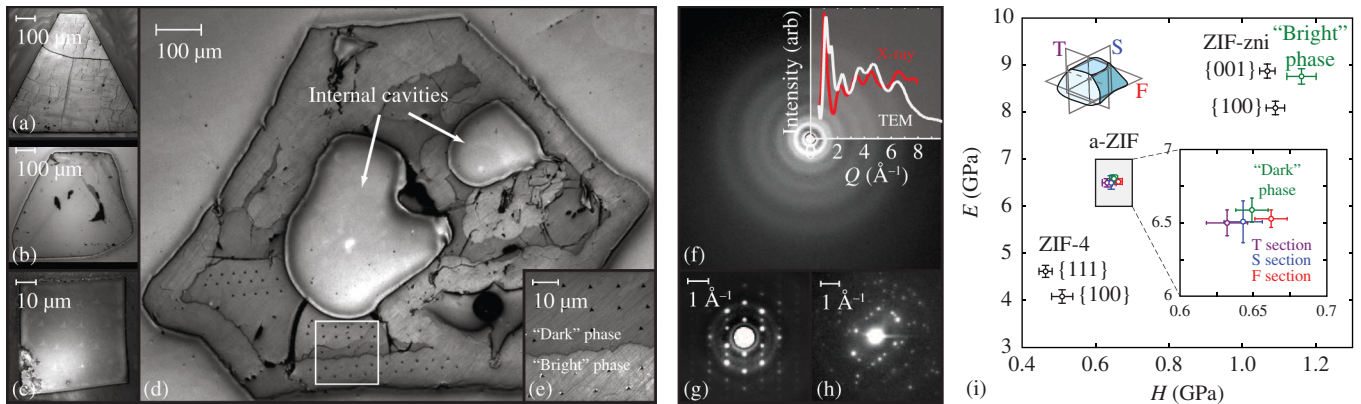

FIG. 4 (color online). Typical optical micrographs of: (a) a desolvated ZIF-4 single crystal, where the desolvation process has induced visible surface cracking; (b) a recovered a-ZIF monolith, showing curved external surfaces and curved internal cavities; (c) a ZIF-zni single crystal prepared independently (see SI for further details); (d), (e) a partially recrystallized monolith consisting of a-ZIF ("dark") and ZIF-zni ("bright") phases—panel (e) is that portion of the monolith in (d) enclosed within the white square and shows the indentations used to measure mechanical behavior of the two phases [30]. Electron diffraction patterns from: (f) an a-ZIF monolith together with the radially averaged intensity distribution for qualitative comparison with the x-ray scattering function $F_X(Q)$; (g) a crystallite of ZIF-4 prior to heating; (h) a polycrystalline monolith after transformation to ZIF-zni. (i) Young's moduli (E) and hardnesses (H) determined for the different phases in panels (a)–(e) along known orientations, over surface penetration depths of 150 to 1000 nm ("T," "S," "F" refer to the transverse, sagittal, and frontal sections). These measurements were used to assign the dark and bright phases in panel (c) as a-ZIF and ZIF-zni, respectively, indicating that ZIF-zni nucleates at the monolith surfaces during recrystallization.

x-ray diffraction patterns, was stable under beam irradiation to an extent that suggests complete amorphization. Subsequent recrystallization of ZIF-zni during *in situ* heating yields polycrystalline monoliths with submicron grains of random orientation [Fig. 4(h)], suggesting there is no ''memory'' of the original ZIF-4 orientation. In light of these findings, one also expects *a*-ZIF to exhibit mechanical isotropy rather than the anisotropy of the two crystalline phases. We tested this by performing a series of nanoindentation studies [30] on single crystals or monoliths of the ZIF-4, *a*-ZIF and ZIF-zni samples. Elastic moduli and hardness values confirm the loss of anisotropy in the amorphous phase and show the mechanical properties of *a*-ZIF to be intermediate to but distinct from those of ZIF-zni and ZIF-4 [Fig. 4(i)].

That *a*-ZIF is not formed directly from a melt precludes the use of the term ''glass'' in its traditional sense; specifically, there is no glass transition *per se*, and chemical decomposition precedes melting on heating. Nevertheless, it is clear that *a*-ZIF is fundamentally different from the crystalline ZIF phases. An important question to be answered will be why such a phase should form at all. What we do know is that, like their silicate analogues, ZIFs are only metastable (as indeed are many open-framework MOFs), and this will provide some driving force for thermally activated reconstructive transitions. The existence of multiple intermediate structure topologies with similar energies will then favor an amorphous state until the crystalline minimum (ZIF-zni) becomes thermally accessible. It appears that ZIF materials follow their silica analogues in this respect, and indeed similar arguments have been put forward to explain the formation of amorphous covalent organic networks [31].

There is every reason to expect similar amorphization mechanisms in other MOFs. Indeed, we observe this to be the case in ZIFs in which Zn is replaced by magnetic Co (II). It is precisely this chemical variability that means access to glasslike MOFs will offer a number of exciting opportunities in the development of functional amorphous materials. The use of chiral bridging ligands, for example, suggests a method of producing optically active network glasses; likewise, the incorporation of lanthanide metal centers and/or electronically active ligands would be an obvious means of preparing electroluminescent glasses for advanced photonics. Our results here show that the major hurdle faced by the community in developing such systems—namely, access to a method of characterizing and understanding their atomic-scale structures—is no longer insurmountable.

*akc30@cam.ac.uk

 [1] A. L. Greer, Science **267**, 1947 (1995).
 [2] G. N. Greaves and S. Sen, Adv. Phys. **56**, 1 (2007).
 [3] T. P. I. Saragi *et al.*, Chem. Rev. **107**, 1011 (2007).
 [4] C. N. R. Rao, A. K. Cheetham, and A. Thirumurugan, J. Phys. Condens. Matter **20**, 083202 (2008).
 [5] G. Férey, Dalton Trans. **23**, 4400 (2009).
 [6] M. Oh and C. A. Mirkin, Nature (London) **438**, 651 (2005).
 [7] D. Maspoch *et al.*, Nature Mater. **2**, 190 (2003).
 [8] N. Masciocchi *et al.*, Inorg. Chem. **42**, 6147 (2003).
 [9] K. W. Chapman, G. J. Halder, and P. J. Chupas, J. Am. Chem. Soc. **131**, 17546 (2009).
[10] R. Lehnert and F. Seel, Z. Anorg. Allg. Chem. **464**, 187 (1980).
[11] Y. Q. Tian *et al.*, Chem. Eur. J. **9**, 5673 (2003).
[12] R. Banerjee *et al.*, Science **319**, 939 (2008).
[13] G. N. Greaves *et al.*, Nature Mater. **2**, 622 (2003).
[14] K. S. Park *et al.*, Proc. Natl. Acad. Sci. U.S.A. **103**, 10186 (2006).
[15] See supplementary information at http://link.aps.org/supplemental/10.1103/PhysRevLett.104.115503 for details of experimental methods, sample characterization, and structure refinements.
[16] D. W. Lewis *et al.*, Crystal Engineering Communications **11**, 2272 (2009).
[17] N. Masciocchi *et al.*, Inorg. Chem. **40**, 5897 (2001).
[18] N. Masciocchi *et al.*, Inorg. Chem. **40**, 6983 (2001).
[19] A. C. Hannon, Nucl. Instrum. Methods Phys. Res., Sect. A **551**, 88 (2005).
[20] J. te Nijenhuis, M. Gateshki, and M. J. Fransen, Z. Kristallogr. Suppl. **30**, 163 (2009).
[21] D. A. Keen, J. Appl. Crystallogr. **34**, 172 (2001).
[22] D. A. Keen and M. T. Dove, J. Phys. Condens. Matter **11**, 9263 (1999).
[23] M. G. Tucker *et al.*, J. Phys. Condens. Matter **19**, 335218 (2007).
[24] J. Haines *et al.*, J. Am. Chem. Soc. **131**, 12333 (2009).
[25] D. A. Keen *et al.*, Phys. Rev. Lett. **98**, 225501 (2007).
[26] E. C. Spencer *et al.*, J. Am. Chem. Soc. **131**, 4022 (2009).
[27] S. A. Moggach, T. D. Bennett, and A. K. Cheetham, Angew. Chem., Int. Ed. **48**, 7087 (2009).
[28] M. G. Tucker *et al.*, J. Phys. Condens. Matter **17**, S67 (2005).
[29] F. Wooten, K. Winer, and D. Weaire, Phys. Rev. Lett. **54**, 1392 (1985).
[30] J. C. Tan *et al.*, Acta Mater. **57**, 3481 (2009).
[31] J.-X. Jiang *et al.*, Angew. Chem., Int. Ed. **46**, 8574 (2007).